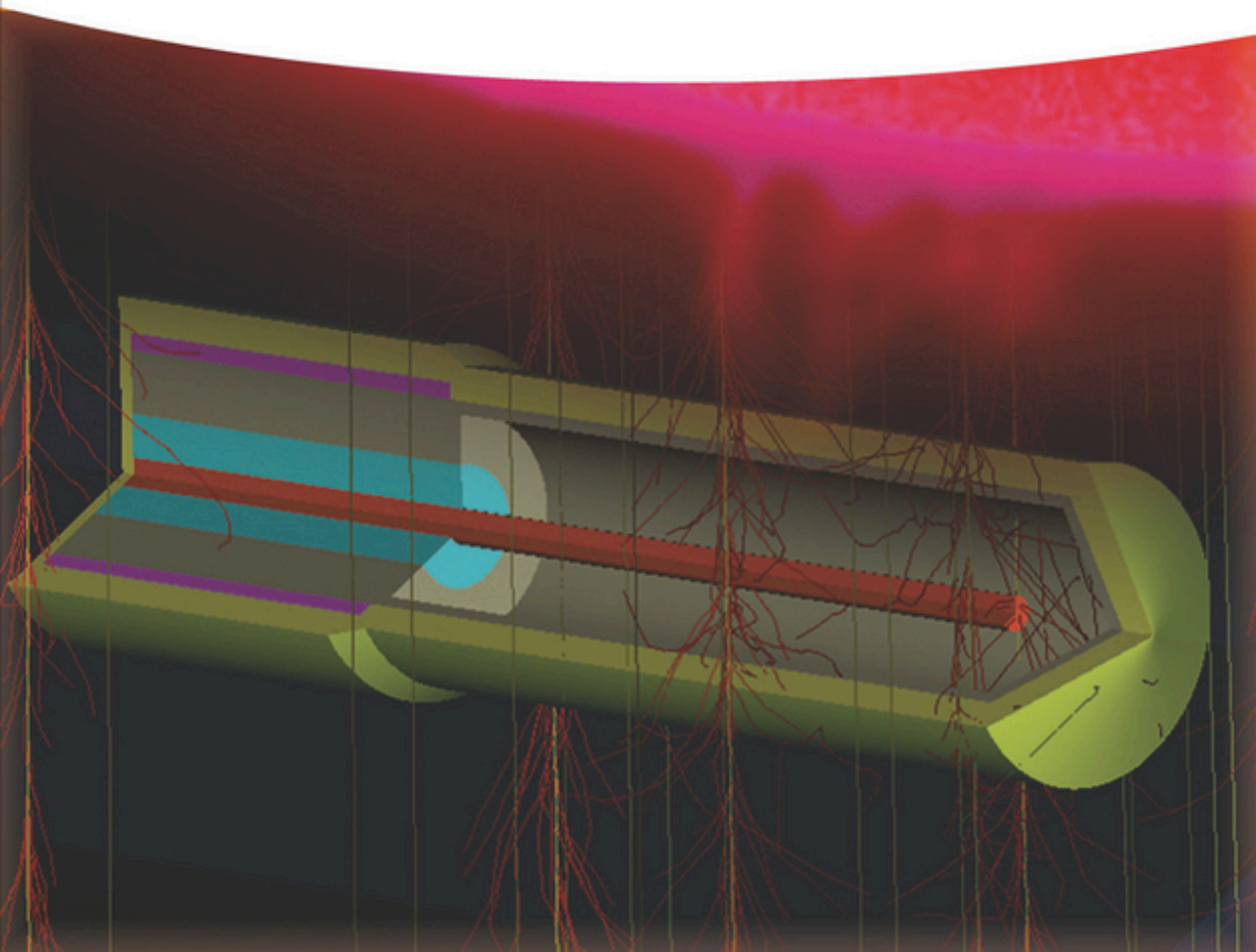


Pedro Andreo, David T. Burns,  
Alan E. Nahum, and Jan Seuntjens

# Fundamentals of Ionizing Radiation Dosimetry

Solutions to the Exercises





## **Fundamentals of Ionizing Radiation Dosimetry**

*Solutions to Exercises*



# **Fundamentals of Ionizing Radiation Dosimetry**

Solutions to Exercises

*Pedro Andreo, David T. Burns,  
Alan E. Nahum, and Jan Seuntjens*

**WILEY-VCH**

## The Authors

**Prof. Pedro Andreo, FlinstP, CPhys**  
Karolinska University Hospital  
171 76 Stockholm  
Sweden

**Dr. David T. Burns, FlinstP**  
Bureau International des  
Poids et Mesures  
Pavillon de Breteuil  
92312 Sèvres Cedex  
France

**Prof. Alan E. Nahum, FIPEM**  
Visiting Professor  
Physics Department  
University of Liverpool  
United Kingdom

**Prof. Jan Seuntjens, FCCPM, FAAPM,  
FCOMP**  
McGill University  
Medical Physics Unit  
Cancer Research Program  
Research Institute  
McGill University Health Centre  
1001 Décarie Blvd  
Montreal QC H4A 3J1  
Canada

## Cover Credits

The cover image was kindly provided by  
Dr Jörg Wulff.

■ All books published by **Wiley-VCH** are carefully produced. Nevertheless, authors, editors, and publisher do not warrant the information contained in these books, including this book, to be free of errors. Readers are advised to keep in mind that statements, data, illustrations, procedural details or other items may inadvertently be inaccurate.

**Library of Congress Card No.:**  
applied for

## British Library Cataloguing-in-Publication Data

A catalogue record for this book is available from the British Library.

## Bibliographic information published by the Deutsche Nationalbibliothek

The Deutsche Nationalbibliothek lists this publication in the Deutsche Nationalbibliografie; detailed bibliographic data are available on the Internet at <<http://dnb.d-nb.de>>

© 2017 Wiley-VCH Verlag GmbH & Co. KGaA, Boschstr. 12, 69469 Weinheim, Germany

All rights reserved (including those of translation into other languages). No part of this book may be reproduced in any form – by photoprinting, microfilm, or any other means – nor transmitted or translated into a machine language without written permission from the publishers. Registered names, trademarks, etc. used in this book, even when not specifically marked as such, are not to be considered unprotected by law.

**Print ISBN:** 978-3-527-34352-2

**ePDF ISBN:** 978-3-527-81106-9

**ePub ISBN:** 978-3-527-81104-5

**Mobi ISBN:** 978-3-527-81105-2

**Typesetting** SPi Global, Chennai, India  
**Printing and Binding**

Printed on acid-free paper

## Contents

	Preface	<i>vii</i>
1	Background and Essentials	1
2	Charged Particle Interactions	5
3	Uncharged Particle Interactions with Matter	23
4	Field and Dosimetric Quantities and Radiation Equilibrium: Definitions and Interrelations	35
5	Elementary Aspects of the Attenuation of Uncharged Particles through Matter	47
6	Macroscopic Aspects of the Transport of Radiation through Matter	53
	Implementation	54
	Normalization of Results	55
7	Characterization of Radiation Quality	57
8	The Monte Carlo Simulation of the Transport of Radiation through Matter	69
9	Cavity Theory	85
10	Overview of Radiation Detectors and Measurements	93
11	Primary Radiation Standards	99
12	Ionization Chambers	109
13	Chemical Dosimeters	117

- 14     **Solid-State Dosimeters**    *123*
- 15     **Reference Dosimetry for External Beam Radiation  
Therapy**    *129*
- 16     **Dosimetry of Small and Composite Radiotherapy Photon  
Beams**    *143*
- 17     **Reference Dosimetry for Diagnostic and Interventional  
Radiology**    *145*
- 18     **Absorbed-Dose Determination for Radionuclides**    *153*
- 19     **Neutron Dosimetry**    *169*



## Preface

The first edition of Frank Herbert Attix's widely used book *Introduction to Radiological Physics and Radiation Dosimetry* was published in 1986 and reprinted in 2004. The exercises and solutions at the end of each chapter were widely regarded as a useful complement to the theory described in the different chapters.

In the second edition of the book, which we abbreviate as FIORD (from *Fundamentals of Ionizing Radiation Dosimetry*), the exercises have been updated and new ones prepared for chapters and topics that were not included in the first edition. Publishing the solutions to the exercises as a separate book was considered to be a more convenient approach, and they are presented here in order to complement some of the (sometimes limited) discussions in the textbook, supported by references to its equations and figures. Hopefully, they will also be a source of inspiration for teachers to prepare new exercises.

The electronic Data Tables of the textbook, necessary for the solution of the exercises, are available from <http://www.wiley-vch.de/ISBN9783527409211>; physical constants and atomic data are also given in Appendix A of the textbook.

6th December 2016

*Pedro Andreo  
David T. Burns  
Alan E. Nahum  
Jan Seuntjens*



## 1

## Background and Essentials

- 1 What is the photon energy range corresponding to the UV radiation band?

*Answer: 10 nm–400 nm corresponds to 124 eV–3.1 eV.*

**Solution:**

The quantum energy  $k$  of any electromagnetic photon is given in keV by

$$k = h\nu = \frac{hc}{\lambda} = \frac{12.3982 \text{ keV } \text{\AA}}{\lambda} = \frac{1.23982 \text{ keV nm}}{\lambda}$$

where  $1 \text{ \AA}(\text{Angstrom}) = 10^{-10} \text{ m}$ , Planck's constant is  $h = 6.62607 \times 10^{-34} \text{ J s} = 4.13561 \times 10^{-18} \text{ keV s}$  (note that  $1.6022 \times 10^{-16} \text{ J} = 1 \text{ keV}$ ), and the velocity of light in vacuum is  $c = 2.99792 \times 10^8 \text{ m/s} = 2.99792 \times 10^{18} \text{ \AA/s} = 2.99792 \times 10^{17} \text{ nm s}^{-1}$ .

Therefore for the UV radiation, which is in the range of 10 nm–400 nm, the equation yields 124 eV–3.1 eV.

- 2 For a kinetic energy of 100 MeV, calculate the velocity  $\beta$ , for (a) electrons, (b) protons, and (c) alpha particles. The corresponding rest energies are given in the Data Tables.

*Answer: (a) 0.9999; (b) 0.4282; (c) 0.2271*

**Solution:**

We can apply either of the relations

$$\beta^2 = \frac{\tau(\tau + 2)}{(\tau + 1)^2}, \quad \text{with } \tau = E/m_0c^2$$

or

$$\beta^2 = \frac{E(E + 2m_0c^2)}{(E + m_0c^2)^2}$$

From the Data Tables, the rest energies are  $m_e c^2 = 0.51099 \text{ MeV}$ ,  $m_p c^2 = 938.272 \text{ MeV}$ , and  $m_\alpha c^2 = 3727.38 \text{ MeV}$ . These yield

- (a) Electrons: 0.9999  
 (b) Protons: 0.4282  
 (c) Alpha particles: 0.2271

- 3 Conversely given a value of  $\beta = 0.95$ , calculate the corresponding kinetic energies of electrons, protons, and  $\alpha$  particles.

Answer: (a) 1.1255 MeV; (b) 2066.6 MeV; (c) 8209.86 MeV

**Solution:**

The relation between the kinetic energy and the speed ( $\beta$ ) is

$$E = \frac{m_0 c^2 \beta^2}{2\sqrt{1 - \beta^2}}$$

Using the rest energies from the previous exercise, we get

- (a) Electrons: 1.1255 MeV  
 (b) Protons: 2066.6 MeV  
 (c)  $\alpha$ -particles: 8209.86 MeV
- 4 The result of a given process is derived as the product of several independent quantities,  $Q = \prod q_i$ . The type A and B uncertainties of each  $q_i$ ,  $(u_A, u_B)_i$ , given as a relative standard uncertainty, are (0.1, 0.5), (0.01, 0.1), (0.02, 0.4), and (0.3, 0.19). Determine the combined standard uncertainty of  $Q$ .

Answer:  $u_c(Q) = 0.75$

**Solution:**

Use the *law of propagation of uncertainty* twice: first for each of the respective types of uncertainty to yield the overall  $u_A$  and  $u_B$  types,

$$u_A = \sqrt{\sum_i u_{A_i}^2}, \quad u_B = \sqrt{\sum_i u_{B_i}^2}$$

and then for the combination of these two to yield  $u_c(Q)$ .

Hence

Quantity	Rel standard uncertainty	
	$(u_A)_i$	$(u_B)_i$
$q_1$	0.10	0.50
$q_2$	0.01	0.10
$q_3$	0.02	0.40
$q_4$	0.30	0.19
Combined	$u_A = 0.32$	$u_B = 0.68$

resulting in a combined uncertainty

$$u_c(Q) = \sqrt{u_A^2 + u_B^2} = 0.75$$

- 5 Given the following set of data (75.4, 79.7, 75.0, 77.0, 78.4), with standard uncertainties (0.95, 0.5, 0.2, 1.2, 0.8), (a) determine the non-weighted and weighted means and the corresponding type A uncertainties. (b) Determine the Birge ratio for the data and comment on the uncertainty estimates of the data.

Answer:  $\bar{x} = 77.1$ ,  $s_{\bar{x}} = 0.89$ ;  $\bar{x}_w = 75.8$ ,  $s_{\bar{x}_w} = 0.18$ ;  $R_{\text{Birge}} = 2.2$

**Solution:**

(a) Requires the straightforward application of Eqs. (1.41)–(1.46), where the different terms are

$i$	$x_i$	$(x_i - \bar{x})^2$	$s_i$	$w_i (= 1/s_i^2)$	$w_i x_i$	$w_i(x_i - \bar{x}_w)^2$
1	75.4	2.89	0.95	1.11	83.55	0.18
2	79.7	6.76	0.50	4.00	318.80	60.79
3	75.0	4.41	0.20	25.00	1875.00	16.07
4	77.0	0.01	1.20	0.69	53.47	1.00
5	78.4	1.69	0.80	1.56	122.50	10.55
$n$	$\sum_i x_i$	$\sum_i (x_i - \bar{x})^2$		$\sum_i w_i$	$\sum_i w_i x_i$	$\sum_i w_i (x_i - \bar{x}_w)^2$
5	385.5	15.8		32.36	2453.32	88.58
Eqs	(1.41)	(1.43)		(1.45)	(1.44)	(1.46) num
	$\bar{x}$	$s(\bar{x})$		$s(\bar{x}_w)_{\text{int}}$	$\bar{x}_w$	$s(\bar{x}_w)_{\text{ext}}$
	77.10	0.89		0.18	75.80	0.83

(b) The Birge ratio is given by

$$R_{\text{Birge}} = \frac{s(\bar{x}_w)_{\text{int}}}{s(\bar{x}_w)_{\text{ext}}} = 2.2$$

$R_{\text{Birge}} = 2.2$  is a sign that some uncertainties have been under/over estimated. We typically think that we can make estimates at, say, the 20% level. A Birge significantly greater than 1.2 or 1.3 is a reasonable sign of under/overestimation. However, one proviso is the balance of uncertainties. One huge under/overestimate can make Birge large even if other uncertainties are properly estimated, especially for small data sets. This could be the case with data #3, where  $s = 0.20$  might be an underestimation.

- 6 Using the half-width of the set of data in the previous exercise, estimate the type B uncertainty assuming rectangular, triangular, and Gaussian (with  $k = 2$ ) distributions. Which of the three is considered to be more conservative?

*Answer:  $u_{B \text{ rect}} = 1.36$ ,  $u_{B \text{ trian}} = 0.96$ ,  $u_{B \text{ Gauss}} = 1.18$ ; the 95% Gaussian is more conservative.*

**Solution:**

The half-width of the set of data,  $[-L, +L]$ , is determined as

$$L = \frac{\max(x_i) - \min(x_i)}{2} = \frac{79.7 - 75.0}{2} = 2.35$$

Hence

$$u_{B, \text{rect}} = \frac{L}{\sqrt{3}} = \frac{2.35}{1.73} = 1.36$$

$$u_{\text{B,triang}} = \frac{L}{\sqrt{6}} = \frac{2.35}{2.45} = 0.96$$

$$u_{\text{B,95\%}} = \frac{L}{2} = \frac{2.35}{2} = 1.18$$

The rectangular distribution is a special case, because in general for most data sets there is a higher probability that the true value lies nearer to the middle than at the extremes. This leaves the triangular and Gaussian ( $k = 2 \rightarrow 95\%$ ) distributions being conceptually similar, with the 95% Gaussian being more conservative.

2

**Charged Particle Interactions**

- 1 For the Rutherford (Geiger and Marsden) experiment with 5.5 MeV  $\alpha$  particles on a 1  $\mu\text{m}$  gold foil and for the six angles (decades) between  $10^{-5}$  and  $10^0$  rad, calculate the Rutherford differential cross section (DCS),  $d\sigma_R/d\Omega$ , (a) without and (b) with screening. Represent both results graphically and draw conclusions.

*Answer: The non-screened DCS values vary between  $1.7137 \times 10^{-3}$  and  $2.0273 \times 10^{-23} \text{ cm}^2 \text{ rad}^{-1}$  in the interval  $[10^{-5} - 1 \text{ rad}]$ . The screening angle is  $3.7 \times 10^{-3} \text{ rad}$ , and the corresponding screened DCS values vary between  $9.3620 \times 10^{-14}$  and  $2.0273 \times 10^{-23} \text{ cm}^2 \text{ rad}^{-1}$ . The screening  $\chi_a$  cuts off the otherwise increasing DCS with decreasing angle, which remains practically constant below  $\chi_a$ .*

**Solution:**

Note that the foil thickness is irrelevant, as the interaction is assumed to be with one atom of gold,  $Z = 79$ . The  $\alpha$ -particle charge is  $z = 2$ .

- (a) The non-screened Rutherford DCS is given by

$$\frac{d\sigma_R}{d\Omega} = r_e^2 (z Z)^2 \left( \frac{m_e c^2}{m_0 c^2} \right)^2 \frac{1 - \beta^2}{\beta^4} \frac{1}{(1 - \cos \theta)^2}$$

where the relevant constants given in the Data Tables are  $m_e c^2 = 0.51099 \text{ MeV}$ ,  $m_0 c^2 = m_\alpha c^2 = 3727.38 \text{ MeV}$ ,  $r_e = 2.81794 \times 10^{-13} \text{ cm}$ , and  $\beta^2 = \tau(\tau + 2)/(\tau + 1)^2$  with  $\tau = E/m_\alpha c^2$ . This yields  $\beta = 0.05426$ . The DCS can then be calculated; the results are given in the table below.

- (b) The screened Rutherford DCS is given by

$$\frac{d\sigma_R}{d\Omega} = (z Z r_e)^2 \left( \frac{m_e c^2}{m_0 c^2} \right)^2 \frac{1 - \beta^2}{\beta^4} \frac{1}{(1 - \cos \theta + 0.5 \chi_a^2)^2},$$

which differs from the non-screened DCS in the screening angle  $\chi_a$  in the denominator. This is taken to be that of Molière, which is given by

$$\chi_a^2 = \chi_0^2 \left[ 1.13 + 3.76 \left( \frac{z Z}{137 \beta} \right)^2 \right]$$

where

$$\chi_0 = \frac{4.2121 \times 10^{-3} \sqrt{1 - \beta^2}}{m_0 c^2 \beta} Z^{1/3}$$

Thus the screening values obtained are

$$\chi_0 = 8.922 \times 10^{-5} \text{ rad} \quad (0.005^\circ)$$

$$\chi_a = 3.678 \times 10^{-3} \text{ rad} \quad (0.211^\circ),$$

which can be inserted in the screened DCS and its values obtained. Putting together the results for the two DCS, we get the following table:

$\theta(\text{rad})$	Rutherford DCS ( $\text{cm}^2 \text{rad}^{-1}$ )	
	Non-screened	Screened
$10^{-5}$	$1.7137 \times 10^{-3}$	$9.3620 \times 10^{-14}$
$10^{-4}$	$1.7137 \times 10^{-7}$	$9.3483 \times 10^{-14}$
$10^{-3}$	$1.7137 \times 10^{-11}$	$8.1178 \times 10^{-14}$
$10^{-2}$	$1.7137 \times 10^{-15}$	$1.3296 \times 10^{-15}$
$10^{-1}$	$1.7165 \times 10^{-19}$	$1.7119 \times 10^{-19}$
$10^0$	$2.0273 \times 10^{-23}$	$2.0273 \times 10^{-23}$

which is shown in Figure 2.1 and shows the influence of screening, which at about  $4 \times 10^{-3}$  rad cuts the otherwise increasing DCS with angle, remaining practically constant below  $\chi_a$ .

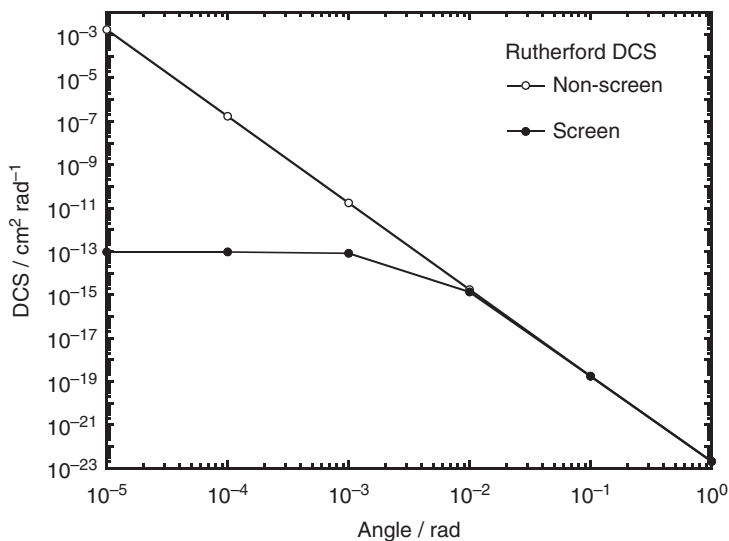


**Figure 2.1** Rutherford differential cross section, with and without screening, for 5.5 MeV  $\alpha$ -particles on a 1  $\mu\text{m}$  gold foil.



- 2 Assume the Rutherford experiment to have been made with protons having the same speed ( $\beta$ ) than the original 5.5 MeV  $\alpha$  particles. Calculate the screened Rutherford DCS for the same angles as above. Compare graphically with the case of  $\alpha$  particles from the previous exercise and draw conclusions.

*Answer: In this case the screening angle is  $\sim 7 \times 10^{-3}$  rad, almost double than that for  $\alpha$  particles with the same  $\beta$ , and the DCS varies between  $2.3635 \times 10^{-14}$  and  $7.9977 \times 10^{-23}$  in the interval  $[10^{-5} - 1 \text{ rad}]$ . The DCS of protons is, above the screening angle, larger than that of the  $\alpha$  particles, as expected from the lower proton rest energy. The larger screening angle for protons, due also to the  $1/m_0c^2$  dependence of  $\chi_0$ , cuts off the DCS earlier (when decreasing angle) than for  $\alpha$  particles, so that for  $\theta < \chi_a$ ,  $DCS_{\text{proton}} < DCS_{\text{alpha}}$ .*

**Solution:**

The constants and expressions to be used are the same as in the previous exercise, with the exception of  $m_p c^2 = 938.272 \text{ MeV}$  and  $z = 1$ . As above,  $\beta = 0.05426$ , which corresponds to a proton energy of 1.384 MeV.

In this case the screening values are

$$\chi_0 = 3.544 \times 10^{-4} \text{ rad} \quad (0.020^\circ)$$

$$\chi_a = 7.313 \times 10^{-3} \text{ rad} \quad (0.419^\circ)$$

which when inserted in the expression for the screened DCS give

$\theta(\text{rad})$	Rutherford DCS ( $\text{cm}^2 \text{ rad}^{-1}$ )
	Screened
$10^{-5}$	$2.3635 \times 10^{-14}$
$10^{-4}$	$2.3626 \times 10^{-14}$
$10^{-3}$	$2.2775 \times 10^{-14}$
$10^{-2}$	$2.8701 \times 10^{-15}$
$10^{-1}$	$6.7005 \times 10^{-19}$
$10^0$	$7.9977 \times 10^{-23}$

Figure 2.2 compares the DCS for protons and for the  $\alpha$  particles from the previous exercise. The figure shows that, above the screening angle, the DCS is larger for protons than for  $\alpha$  particles, as expected from the lower proton rest energy. The larger screening angle for protons ( $\sim 7.3 \times 10^{-3}$  rad) than for  $\alpha$  particles ( $\sim 4 \times 10^{-3}$  rad), due also to the  $1/m_0c^2$  dependence of  $\chi_0$ , cuts off the DCS earlier (when decreasing angle) than in the alpha case, and from that point downward, the DCS is smaller for protons than for the  $\alpha$  particles whenever  $\theta < \chi_a$ .

- 3 (a) Derive an expression for the relativistic screened Rutherford total cross section (TCS) restricted to angles smaller than the atomic screening angle  $\chi_a$ . (b) Compare with the unrestricted expression (Eq. (2.15)) for 5 MeV

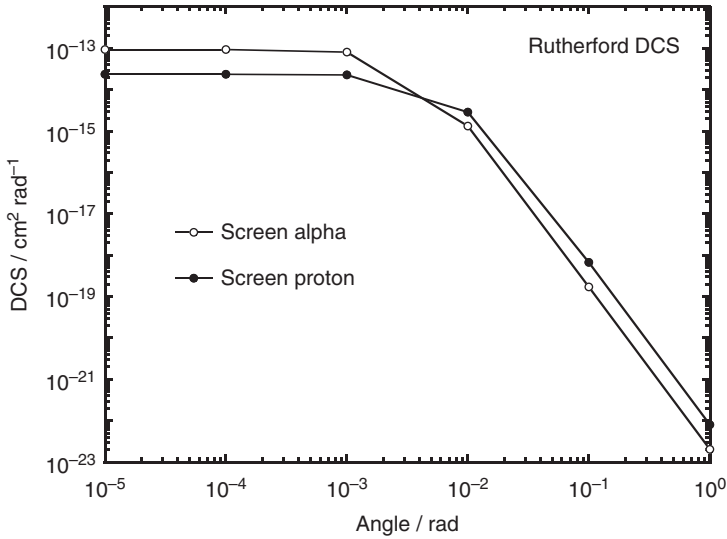


**Figure 2.2** Screened Rutherford differential cross section for protons and  $\alpha$  particles having the same speed  $\beta$ , incident on a  $1 \mu\text{m}$  gold foil.

electrons incident on a mercury atom. (c) Calculate the mean free path of these electrons due to elastic collisions and the subsequent number of elastic collisions per path length.

*Answer:* (a)  $\sigma_R[0, \chi_a] = (z Z r_e)^2 \left( \frac{m_e c^2}{m_0 c^2} \right)^2 \frac{1 - \beta^2}{\beta^4} \frac{8\pi(1 - \cos \chi_a)}{\chi_a^2(2 + \chi_a^2 - 2\cos \chi_a)}$ .

(b)  $\sigma_R[0, \pi] = 2.10731 \times 10^{-18} \text{cm}^2$  and  $\sigma_R[0, \chi_a] = 1.05366 \times 10^{-18} \text{cm}^2$ , that is, elastic collisions with  $\theta \leq \chi_a$  account for practically 50% of the TCS.  
(c)  $\text{MFP} = 0.12 \mu\text{m}$ , that is, almost 10 elastic collisions occur per micron.

**Solution:**

(a) The screened Rutherford DCS is given by

$$\frac{d\sigma_R}{d\Omega} = (z Z r_e)^2 \left( \frac{m_e c^2}{m_0 c^2} \right)^2 \frac{1 - \beta^2}{\beta^4} \frac{1}{(1 - \cos \theta + 0.5 \chi_a^2)^2}$$

where  $\chi_a$  is the screening angle, which in Molière's theory is given by

$$\chi_a^2 = \frac{4.2121 \times 10^{-3} \sqrt{1 - \beta^2}}{m_0 c^2 \beta} Z^{1/3} \left[ 1.13 + 3.76 \left( \frac{z Z}{137 \beta} \right)^2 \right]$$

The screened Rutherford TCS (Eq. (2.15)) was obtained from

$$\begin{aligned} \sigma_R[0, \pi] &= \int_0^\pi \frac{d\sigma_R}{d\Omega} d\Omega = \int_0^\pi \frac{d\sigma_R}{d\Omega} 2\pi \sin \theta d\theta \\ &= (z Z r_e)^2 \left( \frac{m_e c^2}{m_0 c^2} \right)^2 \frac{1 - \beta^2}{\beta^4} \frac{16 \pi}{\chi_a^2(4 + \chi_a^2)} \end{aligned}$$

Instead of integrating in the interval  $[0, \pi]$ , it is convenient to do it in the interval  $[\theta_{\min}, \theta_{\max}]$ , that is,

$$\begin{aligned}\sigma_{\text{R}}[\theta_{\min}, \theta_{\max}] &= \int_{\theta_{\min}}^{\theta_{\max}} \frac{d\sigma_{\text{R}}}{d\Omega} 2\pi \sin \theta \, d\theta \\ &= (z Z r_e)^2 \left( \frac{m_e c^2}{m_0 c^2} \right)^2 \frac{1 - \beta^2}{\beta^4} 2\pi \\ &\quad \left[ \frac{1}{1 - \cos \theta_{\min} + 0.5 \chi_a^2} - \frac{1}{1 - \cos \theta_{\max} + 0.5 \chi_a^2} \right]\end{aligned}$$

which for  $\theta_{\min} = 0$  and  $\theta_{\max} = \pi$  coincides with the expression above. For the present exercise, we then take  $\theta_{\min} = 0$  and  $\theta_{\max} = \chi_a$  and get

$$\begin{aligned}\sigma_{\text{R}}[0, \chi_a] &= \int_0^{\chi_a} \frac{d\sigma_{\text{R}}}{d\Omega} 2\pi \sin \theta \, d\theta \\ &= (z Z r_e)^2 \left( \frac{m_e c^2}{m_0 c^2} \right)^2 \frac{1 - \beta^2}{\beta^4} \frac{8\pi(1 - \cos \chi_a)}{\chi_a^2(2 + \chi_a^2 - 2 \cos \chi_a)}\end{aligned}$$

- (b) For 5 MeV electrons on mercury ( $Z = 80$ ,  $A = 200.59$ ,  $\rho = 13.546 \text{ g cm}^{-3}$ ),  $\beta = 0.995692$ ,  $m_0 c^2 = m_e c^2$ . Thus  $\chi_a = 5.14873 \times 10^{-3} \text{ rad}$  ( $0.3^\circ$ ). Note that we could have replaced  $Z^2$  by  $Z(Z + 1)$ . Therefore

$$\begin{aligned}\sigma_{\text{R}}[0, \pi] &= 2.10731 \times 10^{-18} \text{ cm}^2 \\ \sigma_{\text{R}}[0, \chi_a] &= 1.05366 \times 10^{-18} \text{ cm}^2\end{aligned}$$

that is, elastic collisions with  $\theta \leq \chi_a$  account for practically 50% of the TCS.

The result above explains why even if we would have used the small-angle approximation,

$$\frac{d\sigma_{\text{R,small}}}{d\Omega} = (z Z r_e)^2 \frac{1 - \beta^2}{\beta^4} \frac{4}{(\theta^2 + \chi_a^2)^2}$$

with corresponding TCS

$$\begin{aligned}\sigma_{\text{R,small}}[\theta_{\min}, \theta_{\max}] &= \int_{\theta_{\min}}^{\theta_{\max}} \frac{d\sigma_{\text{R}}}{d\Omega} 2\pi \theta \, d\theta \\ &= (z Z r_e)^2 \frac{1 - \beta^2}{\beta^4} 4\pi \left[ \frac{1}{\theta_{\min}^2 + \chi_a^2} - \frac{1}{\theta_{\max}^2 + \chi_a^2} \right]\end{aligned}$$

that is, for  $\theta_{\max} = 1 \text{ rad}$  and  $\theta_{\max} = \chi_a$ , we get, respectively,

$$\begin{aligned}\sigma_{\text{R,small}}[0, 1] &= (z Z r_e)^2 \frac{1 - \beta^2}{\beta^4} \frac{4\pi}{\chi_a^2(1 + \chi_a^2)}, \\ \sigma_{\text{R,small}}[0, \chi_a] &= (z Z r_e)^2 \frac{1 - \beta^2}{\beta^4} \frac{2\pi}{\chi_a^2},\end{aligned}$$

the results would have been practically identical, as  $\chi_a$  is very small and most collisions occur within  $\theta \leq \chi_a$ .